Application of He I Line Intensity Ratio Method to Tokamak Plasma in TOKASTAR-2*)

Ryoma YOKOYAMA, Atsushi OKAMOTO, Takaaki FUJITA, Hideki ARIMOTO, Masato MINOURA, Kohei YASUDA and Takahiro YAMAUCHI

Graduate School of Engineering, Nagoya University, Furo-cho, Chikusa-ku, Nagoya 464-8603, Japan

(Received 28 December 2017 / Accepted 19 March 2018)

Temporal evolution of electron density and temperature in TOKASTAR-2 tokamak plasma is obtained for the first time by He I line intensity ratio method. In the calculation of collisional radiative model, we consider the effect of radiation trapping and validity of quasi-steady-state approximation for metastable states. He I line intensities are measured using a monochromator that has a photomultiplier tube as a detector. To evaluate line intensity ratios used for analysis, their sensitivity factors for plasma parameters are newly introduced. We investigate plasma current I_p dependence of the electron density n_e and temperature T_e by changing the charging voltage of ohmic heating V_{OH}. The n_e depended on I_p independent of V_{OH}. The Spitzer resistance obtained from the measured T_e was consistent with the plasma resistance at I_p top phase.

© *2018 The Japan Society of Plasma Science and Nuclear Fusion Research*

Keywords: TOKASTAR-2, He I line intensity ratio method, CR model, radiation trapping, tokamak plasma

DOI: 10.1585/pfr.13.3402047

1. Introduction

TOKASTAR-2 is an experimental device which is able to generate tokamak, helical and tokamak-helical hybrid magnetic configurations independently [1]. TOKASTAR-2 device has magnetic field coils in a vacuum vessel (ϕ 0.6 m × 0.6 m) and the plasma has a major radius $R \sim 0.12$ m, a minor radius $a \sim 0.05$ m. In tokamak operation, three coils, Toroidal Field (TF) coil, Ohmic Heating (OH) coil, and Pulsed Vertical Field (PVF) coil, are used. The main purpose of TOKASTAR-2 experiments is to study the effect of helical field on tokamak plasma, which includes stabilization of the plasma position, suppression of disruption, and equilibrium and stability of tokamak-helical hybrid configurations. The electron density, n_e, and the electron temperature, T_e are obtained by using an electrostatic probe method only in helical plasma at present. An electrostatic probe suffers damages due to high heat and particle fluxes in the tokamak plasma in TOKASTAR-2. The plasma current is reduced due to the disturbance of a probe to plasma. To measure n_e and T_e in tokamak plasmas avoiding these problems, we are applying He I intensity ratio method [2, 3] to the tokamak plasma in TOKASTAR-2. The plasma is nonstationary with duration < 0.5 ms of plasma current, I_p. So we developed a measurement system with high temporal resolution.

2. Experimental Setup and Conditions

Experiments were performed using TOKASTAR-2 tokamak plasma. We developed a monochromator measurement system as shown in Fig. 1. It has a photomultiplier tube as a detector. High temporal resolution (10 μs), which is limited by the sampling rate of data logging system, enables us to measure temporal evolution of specific line emission intensities. However, since it measures a single line with a single detector, we have to change the measured wavelength shot by shot assuming reproducibility of the plasma. We measured five He I emission lines (λ = 492.2 nm, 501.6 nm, 667.8 nm, 706.5 nm, and 728.1 nm) as shown in Table 1. We changed voltage of the capacitor for OH coil power supply, V_{OH}, to investigate the plasma current dependence of T_e and n_e. We selected experimental conditions with good plasma reproducibility for each V_{OH} as shown in Table 2, where V_{TF} and V_{PVF} are voltages of the capacitors for TF coil and PVF coil power supply respectively. Temporal evolution of each emission line was

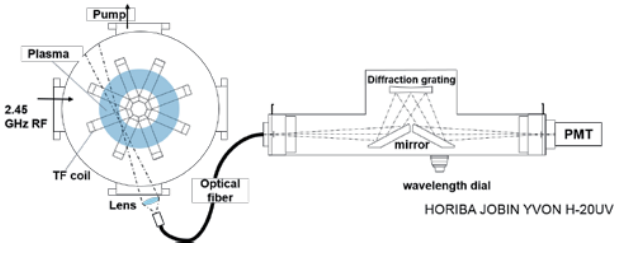

Fig. 1 Monochromator measurement system using HORIBA JOBIN YVON H-20UV.

author's e-mail: okamoto.atsushi@nagoya-u.jp

*) This article is based on the presentation at the 26th International Toki Conference (ITC26).

© 2018 The Japan Society of Plasma Science and Nuclear Fusion Research

Table 1 Observed emission lines.

Wavelength [nm]	Transition
492.193	$2^1\mathrm{P} - 4^1\mathrm{D}$
501.568	$2^1\mathrm{S} - 3^1\mathrm{P}$
667.815	$2^1\mathrm{P} - 3^1\mathrm{D}$
706.518	$2^3\mathrm{P} - 3^3\mathrm{S}$
728.135	$2^1\mathrm{P} - 3^1\mathrm{S}$

Table 2 Experimental conditions.

Working gas	He
Pressure	~ 0.1 Pa
V_{TF}	1.1 kV
V_{OH}	1.6, 1.8, 2.0 kV
V_{PVF}	0.23, 0.26, 0.30 kV

measured under the same experimental conditions.

3. Analysis Methods

To determine n_{e} and T_{e} by spectroscopic method, measured intensity ratios are compared to calculated ones based on the He I collisional-radiative (CR) model for neutral helium atom including the effect of radiation trapping [2, 3].

3.1 Collisional radiative model

This model calculates the population distribution of helium atoms. The temporal evolution of the excited state population density $n(\mathrm{p})$ of a level p is given by the equation below.

$$\begin{aligned}\frac{\mathrm{d}n(p)}{\mathrm{d}t} &= \frac{\partial n(p)}{\partial t} + \nabla \cdot n(p)v \\ &= -\left\{\sum_{q\neq p} C(p,q)n_{\mathrm{e}} + \sum_{q<p} A(p,q) + S(p)n_{\mathrm{e}}\right\} n(p) \\ &\quad + \sum_{q\neq p} C(q,p)n_{\mathrm{e}}n(q) + \sum_{q>p} A(q,p)n(q) \\ &\quad + \{\alpha(p)n_{\mathrm{e}} + \beta(p) + \beta_{\mathrm{d}}(p)\}n_{\mathrm{i}}n_{\mathrm{e}}. \end{aligned} \quad (1)$$

Here $A(p,q)$ is the spontaneous transition probability from p to q, $C(p,q)$ and $S(p)$ are the rate coefficients for electron impact transition (excitation/de-excitation) and electron impact ionization, respectively, and $\alpha(p)$, $\beta(p)$ and $\beta_{\mathrm{d}}(p)$ are the rate coefficients for three-body, radiative, and dielectronic recombination, respectively. The left-hand side is set equal to zero for excited levels except for ground state (quasi-steady-state: QSS approximation). Then, a set of coupled linear equations for $n(p)$ is obtained. By solving it, each excited level population is expressed by a summation of two terms as

$$n(p) = R_0(p)n_{\mathrm{e}}n_{\mathrm{i}} + R_1(p)n_{\mathrm{e}}n(1^1\mathrm{S}), \quad (2)$$

where $R_0(p)$ and $R_1(p)$ are called the reduced population coefficients and are functions of n_{e} and T_{e}.

We investigate validity of QSS approximation for the two metastable states by comparing the transport term on the LHS with the outflow term by electron impact on the RHS in Eq. (1). The transport term is $\nabla \cdot n(p)v = \nabla \cdot \Gamma = -D\nabla^2 n(p) \sim (D/d^2)n(p)$, where Γ is particle flux, D is diffusion coefficient, d is characteristic length concerning density gradient of metastable states. The diffusion coefficient $D = \lambda^2/2\tau$ is of the order of $10^5\,\mathrm{cm^2/s}$, where $\lambda = 1/(n_{\mathrm{n}}\sigma\sqrt{2})$ and $\tau = \lambda/v^{\mathrm{th}}$ are mean free path and mean free time, respectively. We evaluate neutral particle density n_{n} and thermal velocity v^{th} based on the experimental gas pressure ~ 0.1 Pa and temperature 300 K. Assuming $d \sim 10^0$ cm, we obtain $D/d^2 \sim 10^5\mathrm{s}^{-1}$.

The outflow term by electron impact $\sum C(p,q)n_{\mathrm{e}} \sim 10^7\ \mathrm{s}^{-1}$ calculated by the CR model for $n_{\mathrm{e}} = 10^{18}\ \mathrm{m}^{-3}$, $T_{\mathrm{e}} = 10$ eV. Therefore the QSS approximation for the metastable states is valid ($D/d^2 \ll \sum_{q\neq p} C(p,q)n_{\mathrm{e}}$).

To account for the effect of the radiation trapping, we used the optical escape factor (OEF; Λ) that is a function of plasma characteristic length L. In this research, A is replaced with ΛA with value $0 \leq \Lambda \leq 1$. The OEF is evaluated for resonance lines, $1^1\mathrm{S} - n^1\mathrm{P}$ (n = 2, 3,. . .,7). The L becomes an input parameters in addition to n_{e} and T_{e}. These parameters are determined so as to minimize the evaluate function, Eq. (3).

$$f(n_{\mathrm{e}}, T_{\mathrm{e}}, L) = \sqrt{\sum_i \left(\frac{\rho_i^{\mathrm{exp}} - \rho_i^{\mathrm{cal}}}{\rho_i^{\mathrm{exp}}}\right)^2}, \quad (3)$$

where ρ_i^{exp} and ρ_i^{cal} are the i-th specific intensity ratio obtained from the experiment and that from the CR model.

3.2 Sensitivity of line intensity ratios

We investigate sensitivity of line intensity ratios for three parameters: n_{e}, T_{e} and L to decide line intensity ratios used for analysis. In general, to see the sensitivity of line intensity ratios, its contour plot for parameters is used. As an example, contour plots of line intensity ratios proposed by Schweer [4] are shown Fig. 2. The ratio of 667.8 nm and 728.1 nm (blue lines) is nearly parallel to the T_{e} axis. So the ratio doesn't depend on T_{e} and corresponds to n_{e}. The sensitivity of this ratio to n_{e} can be qualitatively seen by the density of contour lines.

In this paper, to quantitatively compare the sensitivity to the parameter of the line intensity ratio, ρ, its sensitivity factor for parameter x was defined:

$$S_x = \left|\frac{\partial\rho}{\partial x}\cdot\frac{x}{\rho}\right| = \left|\frac{\partial\rho/\rho}{\partial x/x}\right|. \quad (4)$$

Here, the line intensity ratio is considered as function of n_{e}, T_{e} and L. So we will see sensitivity factor corresponding to each, $S_{n_{\mathrm{e}}}$, $S_{T_{\mathrm{e}}}$ and S_L as shown in Fig. 3. It is calculated under the conditions of $n_{\mathrm{e}} = 3\times10^{18}\ \mathrm{m}^{-3}$, $T_{\mathrm{e}} = 10$ eV, L = 5 cm except for a parameter of interest.

In Fig. 3 (a), $S_{n_{\mathrm{e}}}$ of 667.8 nm / 728.1 nm is larger than any other line intensity ratios in the n_{e} range of 5×10^{17} - 5

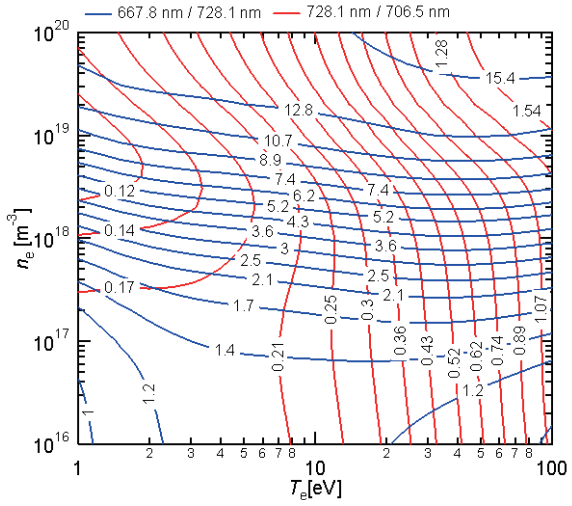

Fig. 2 Contour plots of line intensity ratios against n_e and T_e, assuming $L = 5$ cm.

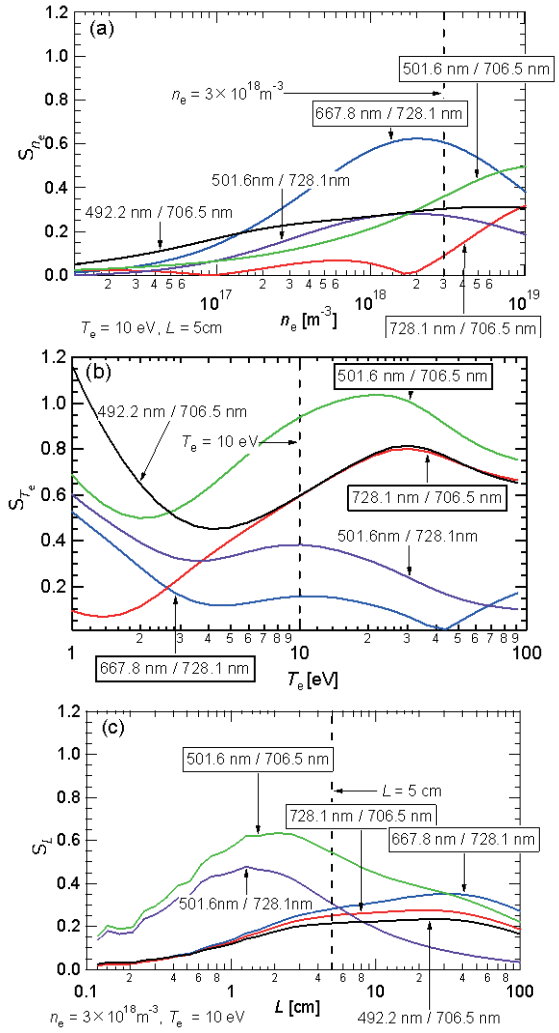

Fig. 3 Sensitivity factor of line intensity ratios for each parameter.

$\times 10^{18}$ m^{-3}. In addition, S_{n_e} of this ratio is larger than other factors: S_{T_e} and S_L. This is consistent with high contour line density and nearly parallel to the T_e axis in that regions of Fig. 3. So this ratio is good for determining n_e. We selected three line intensity ratios for analysis: 667.8 nm / 728.1 nm, 728.1 nm / 706.5 nm and 501.6 nm / 706.5 nm.

4. Results and Discussion

Figure 4 shows that typical temporal evolution of OH coil current, PVF coil current and plasma current. In the tokamak operation, at first, pre-ionized plasma is generated at about 2.3 ms, after injecting RF waves (2.45 GHz) and turning on the TF coil both at 0.45 ms. Then, plasma current is induced by switching on the OH coil power supply at 3.55 ms. In this experiment, the optimum V_{PVF} was selected for each V_{OH}, considering good plasma reproducibility and maximum of plasma current, I_p^{max}. It was found that I_p decreased by about 25 % when V_{OH} was decreased by 10 %, and about 50 % when V_{OH} was decreased by 20 %. Under the same experimental condition we measured the line intensity in 5 shots for each line.

Figure 5 shows temporal evolution of I_p, loop voltage (V_{loop}), T_e and n_e obtained by using selected line intensity ratios as mentioned in sec. 3.2 for each V_{OH}. For I_p and V_{loop} average and standard deviation are taken in 25 shots. The error bars in n_e and T_e are deduced from statistical error in line intensities of each 5 shots. It was found that n_e increases ($< 5 \times 10^{18}$ m^{-3}) and T_e decreases (~ 10 - 20 eV) with time during the current ramp-up phase in all cases of V_{OH} and both n_e and T_e were lower for smaller V_{OH}. The L is about 3 - 10 cm during the plasma pulse in all three cases.

The I_p dependence of T_e and n_e in the current ramp-up phase is shown in Fig. 6. The electron density increases with I_p and its dependency on I_p is nearly independent of V_{OH}. In contrast, the electron temperature decreases or stays constant with increase in I_p and its value at a given I_p is higher for larger V_{OH}.

We discuss consistency between the plasma resistance and the obtained T_e. Table 3 shows the experimental plasma resistance R (= V_{loop}/I_p) and the resistance $R_{SP} = \eta_{SP} l/S$, where $l = 2\pi R_p$ and $S = \pi a_p^2$ are toroidal length and cross section of the plasma for the plasma major radius R_p = 0.115 m and the plasma minor radius a_p = 0.04 m (circular tokamak). η_{SP} is the Spritzer resistivity [6] expressed by

$$\eta_{SP} = 5.2 \times 10^{-5} \frac{Z \ln \Lambda}{T_e^{3/2}[\mathrm{eV}]} \ [\Omega \cdot \mathrm{m}]. \quad (5)$$

Here, $Z = 1$ and Λ are the ion charge number and coulomb logarithm. We assume $T_e = 30$ eV and 10 eV at 3.6 ms and 3.8 ms, respectively. The R and R_{SP} are regarded as consistent at 3.8 ms considering uncertainty in the assumptions, whereas there is two orders of magnitude difference between two resistances at 3.6 ms. Three causes are considered: smaller plasma cross section, the effect of anisotropic

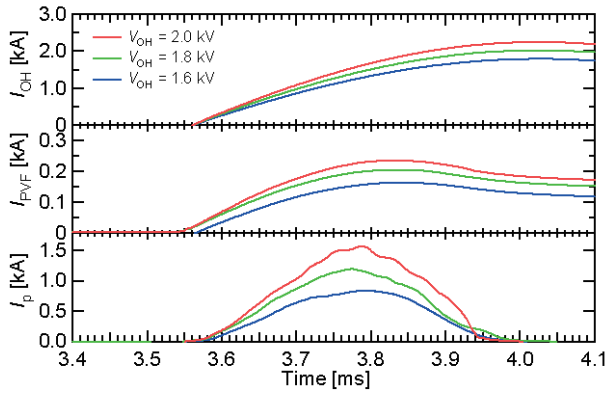

Fig. 4 Typical temporal evolution of I_{OH}, IPVF and I_p.

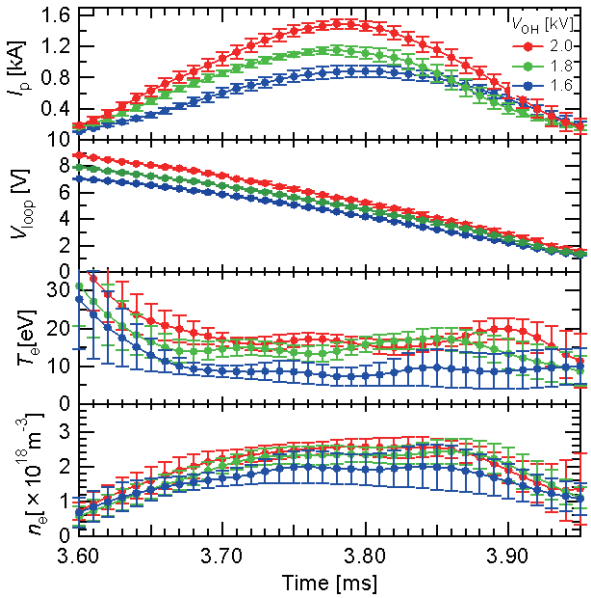

Fig. 5 Temporal evolution of I_p, V_{loop}, T_e and n_e.

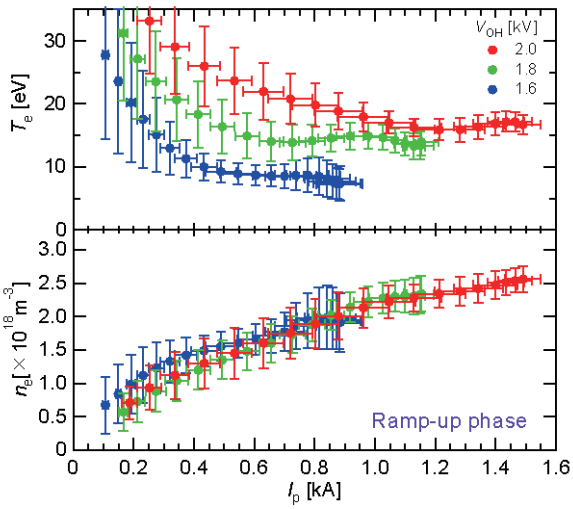

Fig. 6 I_p dependency of T_e and n_e in current ranp-up phase.

Table 3 Plasma resistance.

Time [ms]	R [Ω]	R_{SP} [Ω]
3.6 (I_p^{start})	$\sim 5 \times 10^{-2}$	6.6×10^{-4}
3.8 (I_p^{top})	$\sim 4 \times 10^{-3}$	3.0×10^{-3}

Table 4 Collision frequency.

Time [ms]	T_e [eV]	n_e [m^{-3}]	ν_{en} [s^{-1}]	ν_{ei} [s^{-1}]
3.6	30	1.0×10^{18}	1.96×10^{6}	1.28×10^{5}
3.8	10	2.5×10^{18}	1.38×10^{6}	7.75×10^{5}

electrons in the CR model, and the resistance due to collision of electron with neutral particles. The plasma cross section is estimated to be several times smaller at 3.6 ms than the assumption while it is nearly equal to the assumption at 3.8 ms by the fast camera images. This causes underestimation of R_{SP} at 3.6 ms.

The Maxwellian distribution is assumed in the CR model calculation code used in this study. In Ref. [5], it was shown that population densities in the CR model are strongly affected by the hot electron component. At 3.6 ms, because of the high loop voltage and the low electron density, there is a possibility that electrons are not fully thermalized, or distribution function of electrons is not the Maxwellian distribution. The effect of the loop voltage on the distribution function is, however, not evaluated.

The effect of collision with the neutral particle is evaluated by comparing the collision frequency of electrons with neutral helium atoms ν_{en} and that with singly charged helium ions ν_{ei}. ν_{en} is shown below

$$\nu_{en} = \frac{V_e^{th}}{\lambda_{en}} = V_e^{th} n_n \sigma_{en} = \sqrt{\frac{2k_B T_e}{m_e}} n_n \sigma_{en}, \quad (6)$$

where V_e^{th} [m·s^{-1}] is thermal velocity of electrons, $n_n = 2.4 \times 10^{19}$ m^{-3} is the neutral particle density, λ_{en} [m] is mean free path and $\sigma_{en} = 2.5 \times 10^{-20}$ m^2 is collision cross-section of electron with neutral particles. The collision frequency with the ion is evaluated by the plasma resistivity, $\eta = m_e \nu_{ei}/e^2 n_e$. Using the Spitzer resistivity (Eq. (5)), we obtain $\nu_{ei} = \eta_{SP}(e^2 n_e/m_e)$. We calculated ν_{en} and ν_{ei} from T_e and n_e as shown in Table 4. ν_{en} is about fifteen times as large as ν_{ei} at 3.6 ms, whereas there is only two times differences in both at 3.8 ms. If we consider the effective Spitzer resistivity $\eta^*_{SP} = (1 + \nu_{en}/\nu_{ei})\eta_{SP}$ the value of R_{SP} is modified and become larger. This effect is larger at 3.6 ms than at 3.8 ms.

For detailed discussion, we need quantitative evaluation of the plasma cross-section and of the electron distribution function.

5. Conclusions

Temporal evolution of n_e and T_e in TOKASTAR-2 tokamak plasma was obtained for the first time by He I

line intensity ratio method. In the calculation on the CR model, we considered effect of the radiation trapping and validity of QSS approximation. The He I line intensities were measured using a monochromator that had a photomultiplier tube as a detector. Line intensity ratios used for analysis were decided based on evaluation of their sensitivity factors for plasma parameters of interest. We investigated I_p dependence of n_e and T_e by changing V_{OH}. It was confirmed that n_e depends on I_p independent of V_{OH}. In contrast, T_e decreased or stayed constant with increase in I_p and its value at a given I_p is higher for larger V_{OH}. The Spitzer resistance obtained from the measured T_e was consistent with the plasma resistance at I_p top phase, but the former was two orders of magnitude smaller than the latter at the initial phase.

[1] T. Oishi *et al.*, J. Plasma Fusion Res. SERIES **9**, 69 (2010).
[2] T. Fujimoto, J. Quant. Spectrosc. Radiat. Transf. **21**, 439 (1979).
[3] M. Goto, J. Quant. Spectrosc. Radiat. Transf. **76**, 331 (2003).
[4] B. Schweer *et al.*, J. Nucl. Mater. **196-198**, 174 (1992).
[5] H. Takahashi *et al.*, Contrib. Plasma Phys. **57**, 322 (2017).
[6] F.F. Chen, *Introduction to Plasma Physics and Controlled Fusion*, Vol.1, second edition (Springer Nature, 1983) p.183.